

# Characterization of an Electro-Optical Modulator for Next Linear Collider

## Photocathode Research

Matthew Kirchner

Office of Science, Student Undergraduate Laboratory Internship (SULI)

Colorado School of Mines

Stanford Linear Accelerator Center

Stanford, California

August 11, 2004

Prepared in partial fulfillment of the requirements of the Office of Science, Department of Energy's Science Undergraduate Learning Internship under the direction of A. Brachmann in the Polarized Photocathodes Research Group at Stanford Linear Accelerator Center.

Participant:

\_\_\_\_\_  
Signature

Research Advisor:

\_\_\_\_\_  
Signature

## Table of Contents

	<b>Abstract</b>	iv
<b>1</b>	<b>Introduction</b>	1
<b>2</b>	<b>Theory</b>	2
<b>3</b>	<b>Materials and Methods</b>	4
3.1	Optical Setup	4
3.2	RF Setup	6
3.3	Amplifier Characteristics	6
3.4	Taking Data	7
<b>4</b>	<b>Results</b>	8
4.1	Amplifier Characteristics	8
4.2	Half-wave plate Rotation, DC Bias at 0 and 100 V	10
4.3	DC Bias and Percent Transmittance	12
4.4	Other Tests	12
<b>5</b>	<b>Discussion and Conclusions</b>	13
5.1	Amplifier Characteristics	13
5.2	Half-Wave Plate Rotation, DC Bias at 0 and 100 V	13
5.3	DC Bias	14
5.4	General Conclusions	14
5.5	Opportunities for Further Research	14
	<b>Acknowledgements</b>	15
	<b>Literature Cited</b>	16

## List of Tables

Table 1	A list of constants used for modulator calculations	3
Table 2	Modulator transmittance data showing pulse energy before and after modulator	12

## List of Figures

Figure 1	Diagram of a typical EO modulation setup. Figure from [6]	2
Figure 2	Four crystal modulator setup. Figure from [6]	2
Figure 3	Electrical connections on the electro-optical modulator. Path of the 119 MHz input signal follows the arrows in the diagram.	4
Figure 4	Lens configuration for focusing the beam	5
Figure 5	Schematic of the optical setup	5
Figure 6	Response of the RF amplifier to changes in frequency	9
Figure 7	Response of the RF amplifier to changes in input voltage	9
Figure 8	Graph of data for zero degrees half-wave plate rotation	10
Figure 9	Example of data averaging method showing the actual calculated minimum and maximum values using the given averaging region	10
Figure 10	Percent modulation vs. half-wave plate angle. DC Bias = 0V	11
Figure 11	Percent modulation vs. half-wave plate angle. DC Bias = 100V	11
Figure 12	Laser peak amplitude as seen on oscilloscope vs. DC Bias	12

## **Abstract**

Characterization of an Electro-Optical Modulator for Next Linear Collider Photocathode Research.

MATTHEW KIRCHNER (Colorado School of Mines, Golden, CO, 80401)

AXEL BRACHMANN (Stanford Linear Accelerator Center, Menlo Park, CA, 94025).

The SLAC Next Linear Collider design parameters call for a polarized electron source capable of outputting bunches of electrons 1.4 ns apart (714 MHz). Stanford Linear Accelerator Center (SLAC) currently uses a pulsed Ti:Sapphire laser incident on a GaAs photocathode to produce polarized electrons. The pulses produced by this laser are approximately 300 ns in duration and occur at a frequency of 60 or 120 Hz. The purpose of this research is to find a way to modulate the 300 ns pulse into a high-frequency pulse train. High-frequency modulation of the 300 ns laser pulses was achieved with an electro-optical (EO) modulator, which uses the Pockel's Effect to change the polarization of incoming light. The highest frequency possible was 200 MHz (limited by the RF amplifier). For this reason, the SLAC 119MHz timing signal was selected for input into the amplifier. The output of the amplifier was passed through the EO modulator to induce an alternating half-wave phase shift of the incident laser light. The cube polarizer at the exit of the modulator rejects any laser light not parallel to its polarization axis. These two effects coupled together produce amplitude modulation of the laser pulse. The modulation can be changed by several variables. The linearly polarized light incident into the modulator can be rotated by a half-wave plate to any polarization angle. The DC Bias could be changed to give the RF signal an offset. The input signal can also be changed to vary the voltage across the crystals. Finally, the RF setup (attenuators, splitters, cables, terminators) can be changed. This

paper examines how all of these variables change the modulation characteristics of the EO modulator used. The rotation of the half-wave plate was found to change the percent modulation from 10% to 90%. Adding a DC Bias to the half-wave plate rotation caused the modulated signal to change shape as modulation depth still ranged from 10-90%. The modulation depth was shown to increase with increased input voltage. RF setup was only varied slightly but small changes still gave drastic changes in percent modulation. The EO modulator examined showed that high-frequency modulation of a Ti:Sapphire laser pulse is possible with a high percent modulation. This research should be extended up to 714 MHz and the RF setup should be optimized for maximum modulation in future studies.

## 1. Introduction

A polarized electron source (PES) is needed in accelerator particle physics for certain high energy experiments. Stanford Linear Accelerator Center (SLAC) creates polarized electrons using a Titanium Sapphire (Ti:Sapphire) laser incident on a single-strained layer Gallium Arsenide photocathode [1]. The Ti:Sapphire laser is a pulsed laser, tunable to  $800 \pm 50$  nm wavelength, configured to produce  $\sim 300$  ns pulses of polarized light. These pulses strike the photocathode and produce polarized electrons that are then injected into the linear accelerator for experimentation. This paper describes the generation of a  $\sim 300$  ns long pulse train which will be used for NLC related Research.

One method for attaining a pulse train is to modulate the 300 ns pulse into many shorter sub-pulses using an EO modulator. The device used in this experiment is an electro-optic (EO) modulator (ConOptics, Model 360-80S) and utilizes four Lithium Tantalate (LTA) crystals. LTA has a low intrinsic  $V_{1/2}$  and transmits light in the near infrared wavelength range. By sending an RF signal of appropriate amplitude through the device, it is possible to effect changes in the polarization. These changes are turned into laser pulse modulation by the cube polarizer at the exit of the modulator. A fast photodiode and an oscilloscope are used to measure the laser pulse and its modulation.

This experiment used a 119 MHz RF signal locked to the SLAC master oscillator to modulate the laser beam. Future experiments are planned using a frequency of 714 MHz (according to the SLAC NLC design micro-bunch spacing of 1.4 ns [2]).

The experimental setup and operating conditions of the modulating system, such as RF amplifier characteristics, achieved modular transmission, modulation depth, and the effect of input polarization are described herein.

## 2. Theory

The Model 360-80S modulator uses the Pockels Effect to rotate the polarization of the incident light. The Pockels Effect is a linear electro-optical effect where the induced birefringence in a crystal is proportional to the first power of the applied  $\mathbf{E}$ -field [3] (see Figure 1).

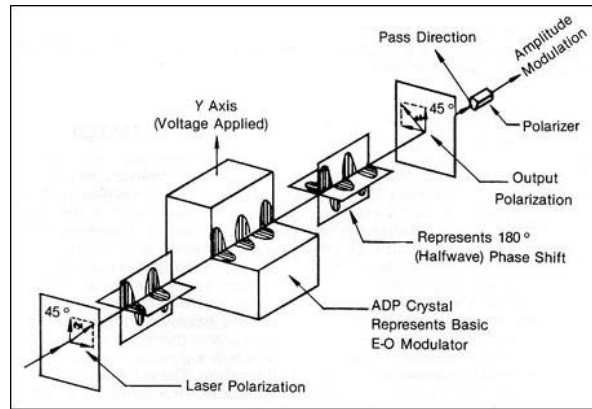


Figure 1. Diagram of a typical EO modulation setup. Figure from [6].

Model 360-80S uses four Lithium Tantalate ( $\text{LiTaO}_3$  or LTA) crystals with a transverse electric field applied by an input voltage as shown in Figure 2.

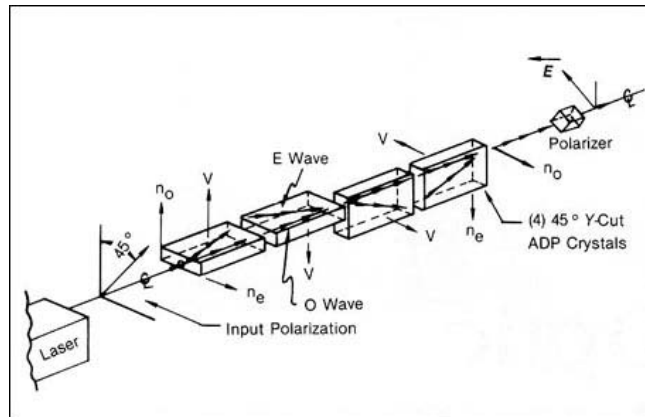


Figure 2. Four crystal modulator setup. Figure from [6]

The phase shift through one of the crystals,  $\Delta\varphi$ , can be expressed as follows [4].

$$\Delta\varphi = 2\pi \frac{Ln^3 r_{33} V}{d\lambda} \quad (1)$$

L is the length of the crystal, d is the width of the crystal or aperture size, n is the ordinary index of refraction,  $r_{33}$  is the electro-optic constant of LTA, V is the applied transverse voltage, and  $\lambda$  is the incident wavelength. Table 1 lists the numerical values of these constants.

Property	Symbol	Value
Length of crystal	L	6.2 mm
aperature/thickness	d	2.7 mm
electro-optical constant	$r_{33}$	30.4 pm/V
ordinary refractive index	$n_o$	2.176
wavelength	$\lambda$	800 nm

**Table 3. A list of constants used for modulator calculations.**

To achieve full modulation, the incident beam must undergo a half-wave phase shift. This means each of the four crystals must give an eighth-wave phase shift. The peak-to-peak voltage into the modulator for the half-wave phase shift is therefore

$$V_{1/2} = \left(\frac{1}{8}\right) \frac{\lambda d}{r_{33} n^3 L} \quad (2)$$

The manufacturer specifies the half-wave voltage at 830 nm to be 143 V [5] and Equation 2 agrees well with a calculated value of 144 V. The calculated value for the half-wave voltage at 800 nm is 139 V.

The high frequency input signal requires specific cable delay between the crystals to achieve the desired modulation because the signal in the cables has a period of the same order of magnitude as typical cable delays. Figure 3 shows the signal propagation in the modulator. If the delay in the cables and crystal is equal to the period of the electrical signal, each crystal should be at the same relative phase of the RF signal and modulation should be a maximum. However, if the delay is half of the RF period, adjacent crystals will be 180 degrees out of phase, resulting in no net modulation. For 119 MHz, the period of oscillation is 8.403 ns; for 714 MHz, the period is

1.401 ns. The manufacturer specifies the crystal delay of .356 ns. Therefore, each cable should have a delay of approximately 8 ns for 119 MHz and approximately 1 ns for 714 MHz.

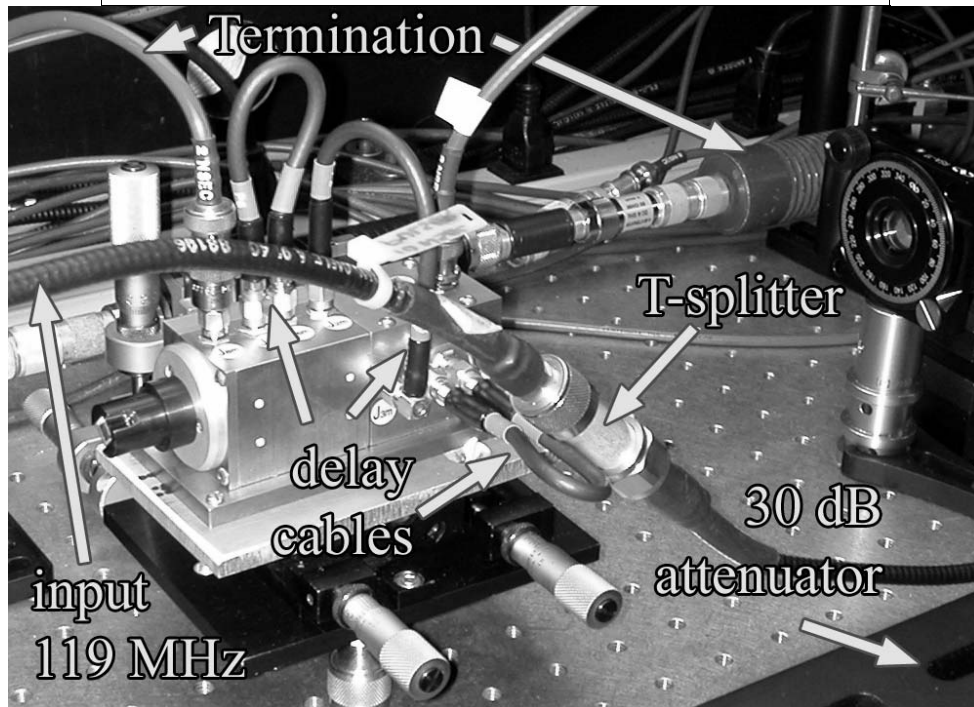
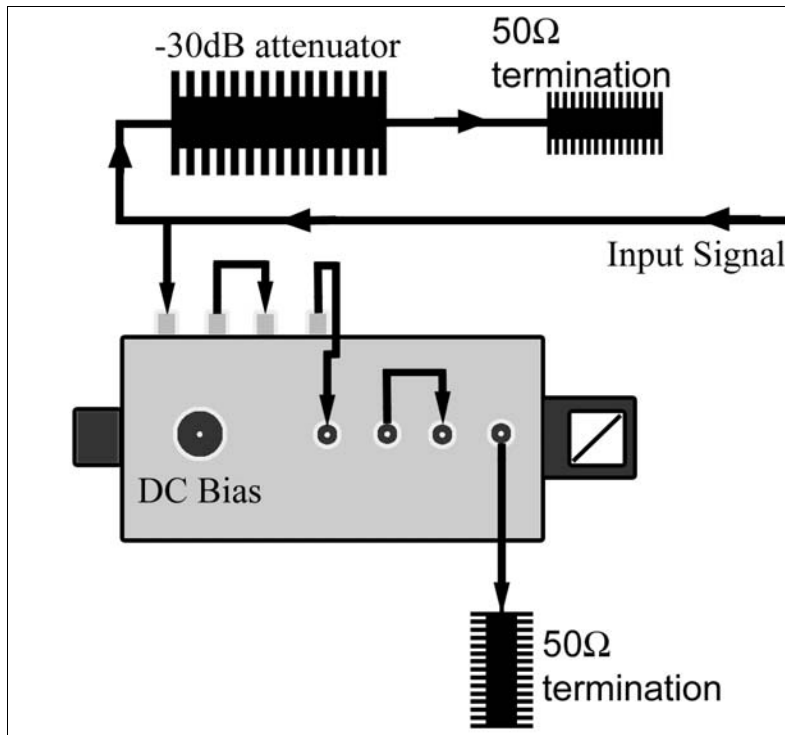


Figure 3. Electrical connections on the electro-optical modulator. Path of the 119 MHz input signal follows the arrows in the drawing.

### 3. Materials and Methods

#### 3.1 Optical Setup

The Ti:Sapphire laser was configured as described in Section 2 of [1]. The beam size, however, was observed to be too large for the 2.7 mm modulator aperture. The small modulator aperture reduces the voltage necessary to effect a half-wave shift (Equation 2), allowing the drive electronics to go faster. Measurements of the beam profile using an adjustable iris and photodiode (UDT, Model 10D 9305-1) showed a beam diameter of approximately 4 mm. A 2:1 telescope was used to focus the beam to approximately 2 mm diameter. David Thomson's Gaussian Beam Calculator program (available for free download from [www.originalcode.com](http://www.originalcode.com)) was used to determine the correct lens focal lengths and lens spacing. This program assumes an ideal Gaussian profile to calculate beam behavior in lenses. The real beam profile is not perfectly Gaussian, so some adjustment of the lens spacing was required. Our final lens configuration is shown in Figure 4.

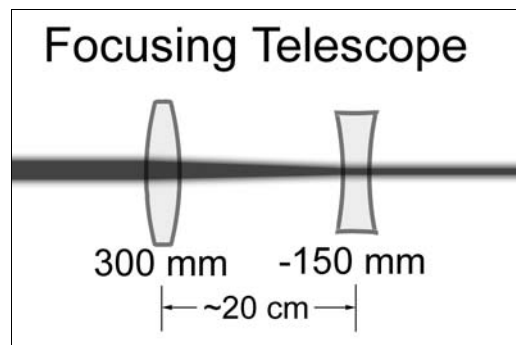
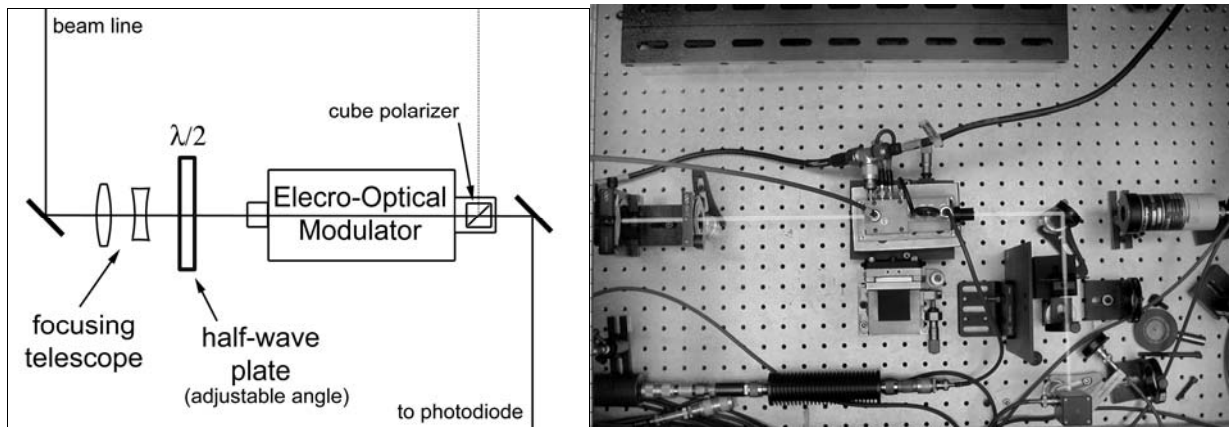


Figure 4. Lens configuration for focusing the beam.

The manufacturer specifies that the exit polarizer is aligned with the crystal axis at 45 degrees with respect to the vertical. The Ti:Sapphire laser beam is vertically polarized making it necessary to position a half-wave plate before the modulator to rotate the beam polarization

(Figure 5). Rotation of the half-wave plate allows for adjustment of transmission through the modulator.



**Figure 5. Schematic of the optical setup.**

The modulator mount was comprised of two adjustable platforms; one that allowed vertical and horizontal displacement and another that gave pitch and yaw adjustments. The modulator was aligned by maximizing the extinction ratio (maximum transmittance divided by minimum transmittance). To do this, the pre-modulator half-wave plate was adjusted to the maximum transmitted signal measured by the slow photodiode and oscilloscope (Tektronix TDS 3054B, 500MHz bandwidth). Then, the position and direction of the modulator were adjusted to further maximize the signal. Next, the half-wave plate was rotated to the transmission minimum and the pitch and yaw of the modulator were varied to reach the absolute minimum. The minimum was recorded and the half-wave plate was then readjusted to the maximum and the extinction ratio was calculated. The maximum extinction ratio achieved was 75:1. The quoted extinction ratio for this model of EO modulator is 60:1.

### **3.2 RF Setup**

The electrical connections were secured to the modulator as shown in Figure 3. For the main data run, the supplied 0.7 ns cables were used to bridge between the crystals. Later tests used 8

ns cables as discussed in Section 3.4. The 119MHz input was taken from the SLAC timing system. This signal was amplified using a large RF amp (Amplifier Research, Model 150A220M3, 150W) and was passed into the modulator. The 119 MHz input signal had to be attenuated slightly so the maximum input of the amplifier (0.5 V peak-to-peak) was not exceeded. The input after attenuation was approximately 0.4 V peak to peak or 140 mV RMS.

### **3.3 Amplifier Characteristics**

The Amplifier Research 150W amplifier is designed for 10 kHz to 200 MHz operation. Measurements were taken of the peak-to-peak amplitude of the output signal using 60 dB total attenuation and the Tektronix oscilloscope. The amplifier response was also measured for a constant 119 MHz input frequency and a variable input voltage.

### **3.4 Taking Data**

The modulation of the laser signal was monitored using a fast photodiode (EOT Silicon PIN detector, Model ET-2000) and the Tektronix oscilloscope. The modulation of the pulse increased with the gain on the amplifier. Maximum modulation was achieved for this amplifier at the maximum gain and the system was left to stabilize. Transient effects on the time scale of a few minutes were observed up to 40 minutes after initial RF amp power-up. Two hours passed before data was taken.

After the stabilization period, the photodiode signal was connected to the HP oscilloscope with computer output capabilities (Hewlett Packard 54522A Oscilloscope, 500 MHz bandwidth). The half-wave plate was set to zero degrees and a single waveform was recorded onto the computer. The wave plate was then rotated five degrees and another waveform was recorded. This was repeated for a total of 180 degrees. Next, the DC bias was set to 100 V and the process was

repeated with ten degree intervals instead of five. The DC bias shortened the stabilization period and data was taken after 45 minutes.

Tests of the DC bias were also performed with the modulation signal turned off. The half-wave plate was adjusted to maximum transmittance at a DC Bias of 0 V. The DC bias was then varied from 0-200 V and pulse height was recorded. The minimum should occur at the half-wave voltage

Finally, the maximum percent transmittance through the modulator was measured. A laser pulse energy meter (Molelectron J3-09, 1.31 V/mJ) was positioned after the modulator and pulse height was maximized by rotation of the half-wave plate and recorded. The energy meter was then placed before the modulator and pulse height was recorded. Dividing the pulse heights gives the percent transmittance.

Further tests of the cable delay and RF setup were undertaken in an attempt to achieve better modulation. The .7 ns cables supplied by the manufacturer were exchanged for 8 ns cables to match the period of our 119 MHz test signal. Attenuators were also placed before the termination of the signal out of the modulator and a change in modulation was observed. Finally, the DC Bias and half-wave plate were adjusted together to attain the best modulation. The results of these tests are discussed in Section 4.4.

## **4. Results**

### **4.1 Amplifier Characteristics**

The output peak-to-peak voltage of the RF amplifier is plotted against input frequency in Figure 6. These values are calculated from the peak-to-peak voltage read by the oscilloscope after 60 dB attenuation. The input signal for each frequency was 100 mV RMS as indicated by the signal

generator (HP 8656B Signal Generator, .1-990 MHz) Figure 7 shows the peak-to-peak voltage output of the amplifier as input voltage was varied from 50-170 mV RMS at 119 MHz.

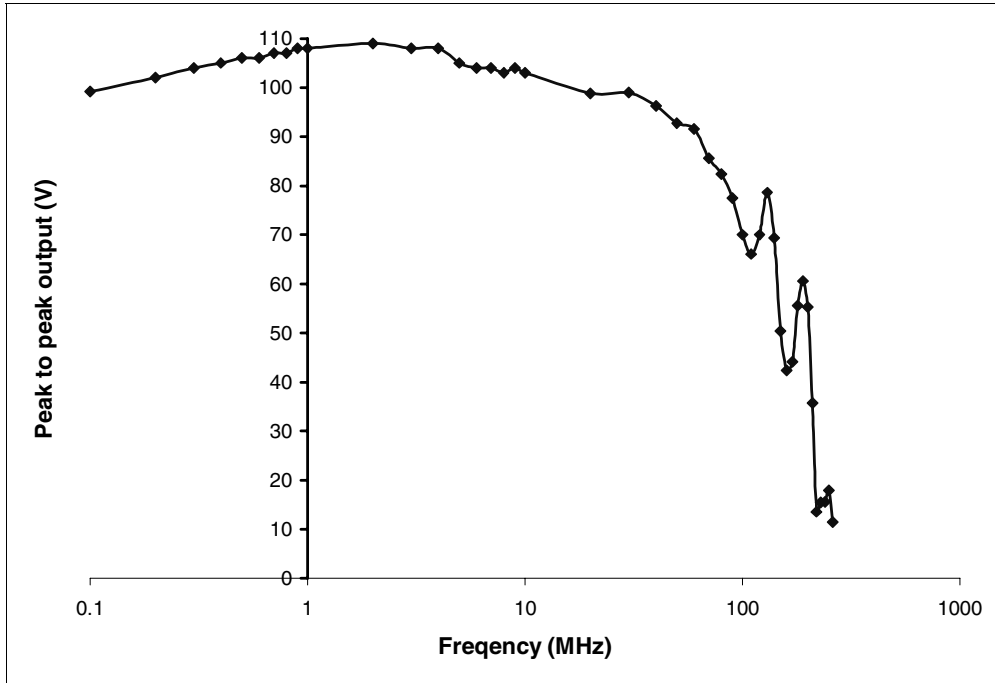


Figure 6. Response of RF amplifier to changes in frequency.  
Note: logarithmic frequency scale

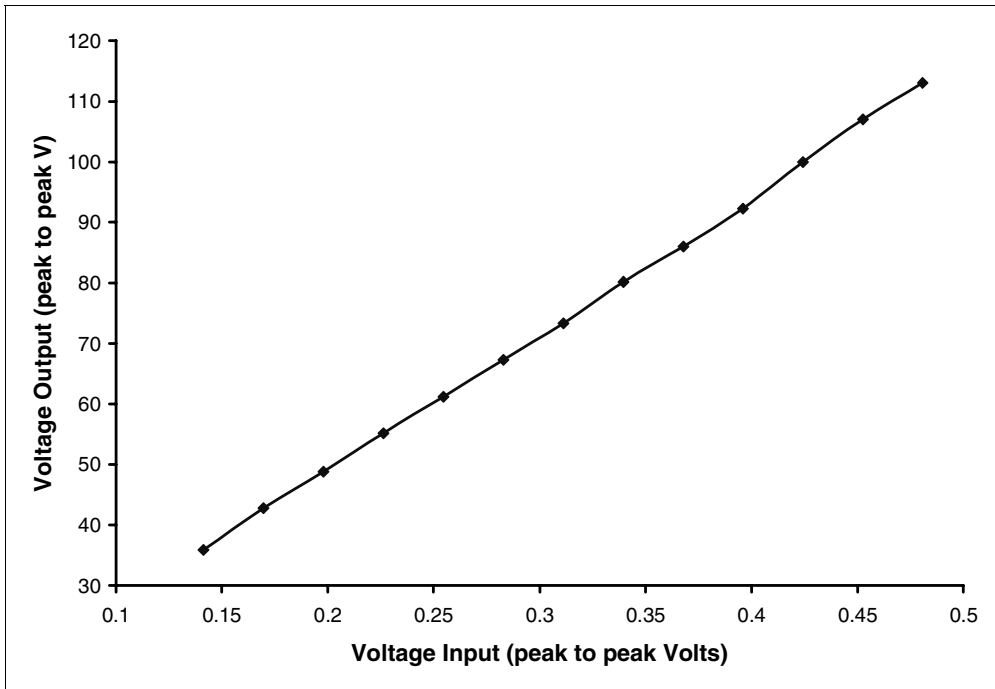
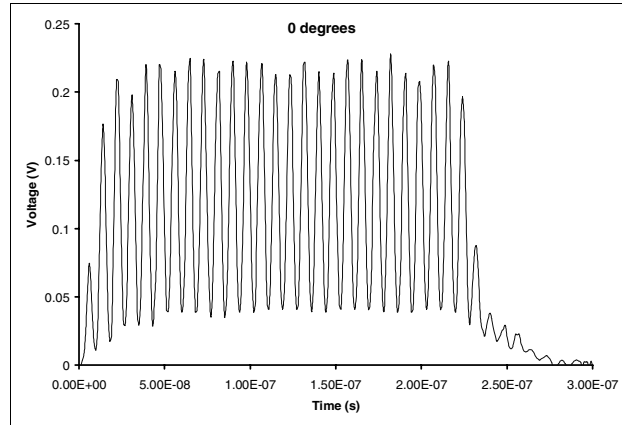


Figure 7. Response of RF amplifier to changes in input voltage.

## 4.2 Half-Wave Plate Rotation, DC Bias at 0 and 100 V

The raw data for each half-wave plate angle was compiled and processed. Figure 8 shows the wave form taken at zero degrees rotation.



**Figure 8. Graph of data for zero degrees half-wave plate rotation.**

Excel was used to find the values of all the local maxima from 100-200 ns. The values for the maxima were then averaged to attain a single averaged value for the maximum of modulation for that angle. The same process was followed to find the averaged minimum. Figure 9 shows a graphical representation of the averaging scheme.

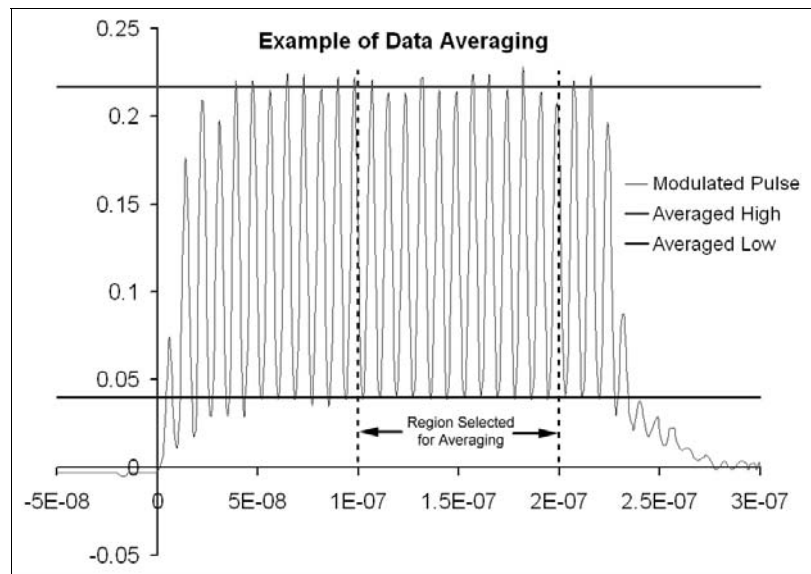


**Figure 9. Example of data averaging method showing the actual calculated minimum and maximum values using the given averaging region.**

Percent modulation was then calculated for each of the angles and plotted to a graph. Figure 10 shows the percent modulation as a function of wave plate angle with a 0 V bias and Figure 11 shows the same for a 100 V bias.

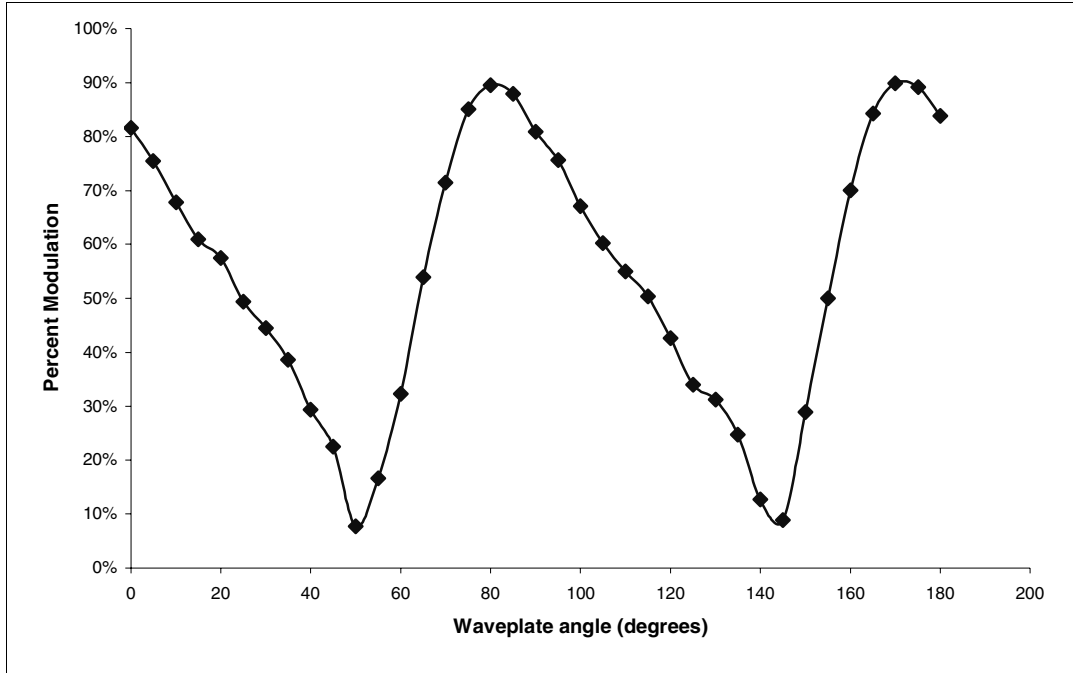


**Figure 10. Percent modulation vs. half-wave plate angle. DC Bias = 0V.**

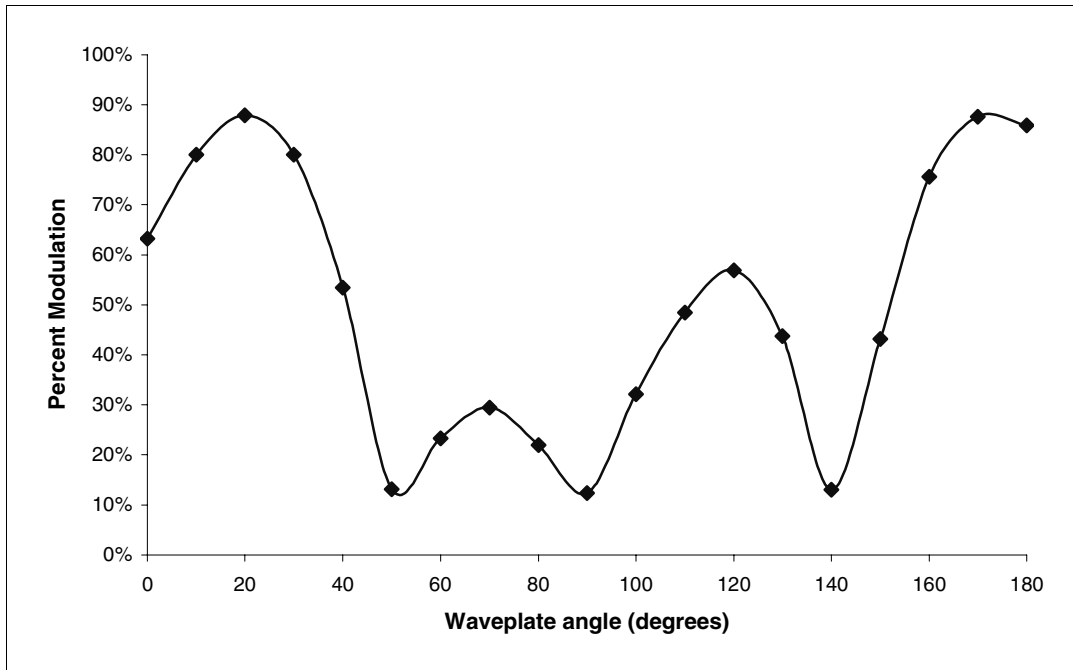


**Figure 11. Percent modulation vs. half-wave plate angle. DC Bias = 100V.**

### 4.3 DC Bias and Percent Transmittance

The data from the DC Bias experiment described in Section 3.4 is summarized in Figure 12.

When a sinusoidal fit is applied to the data, the minimum point is found to occur at 114.7 V.

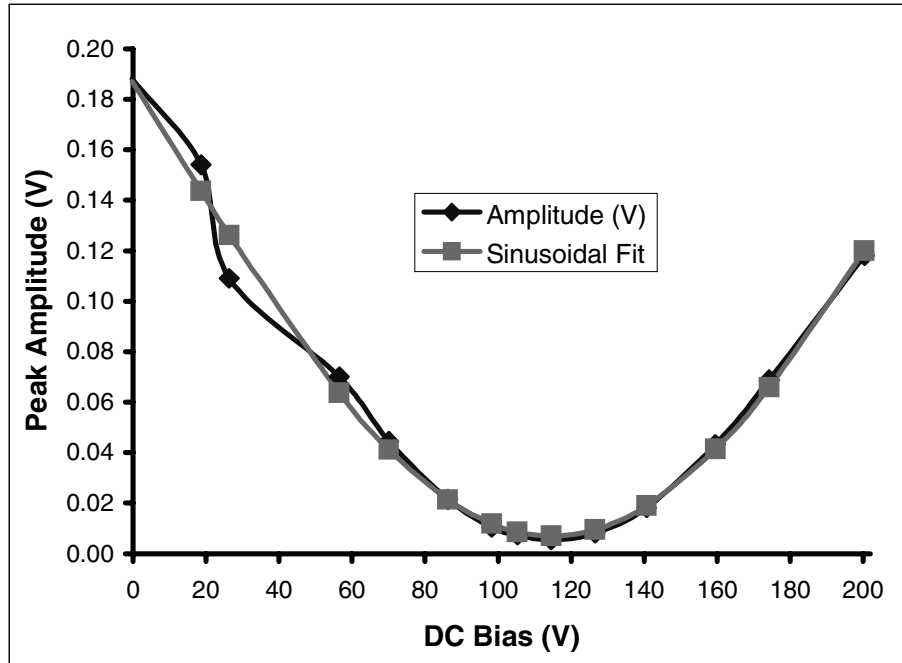


Figure 12. Laser peak amplitude as seen on oscilloscope vs. DC Bias. A sinusoidal fit was made to find the minimum.

The data from the percent transmittance experiment is shown in Table 2. The percent transmittance through the modulator with no voltage applied was found to be 89.8%.

Position	Signal height	Pulse Energy
before modulator	215 mV	164 $\mu$ J
after modulator	193 mV	147 $\mu$ J

Table 4. Modulator transmittance data showing pulse energy before and after modulator

### 4.4 Other tests

Results from switching the cables and changing the RF setup are mostly qualitative because they did not change the modulation to a significant degree. Switching the cables to the correct delay (8 ns) led to no modulation being seen. However, attenuating the output of the modulator for

reading on an oscilloscope increased the modulation dramatically. This indicates that the performance of the modulator can be improved by changes in the RF system setup. The modulation achieved with the attenuators was roughly the same as the modulation with the shorter cables and no attenuators. When the DC Bias and half-wave plate rotation were varied in conjunction, no new results were obtained.

## **5. Discussion and Conclusions**

### **5.1 Amplifier Characteristics**

The frequency response of the amplifier remains flat until around 40 MHz with a maximum around 5 MHz (Figure 6). At higher frequencies the gain drops by a factor of  $\sim 10$  (at 200 MHz). The output response to input voltage at 119 MHz is linear as shown in Figure 7. To compare experiments at different frequencies above 40 MHz, the gain of the amplifier has to be included in the calculations.

### **5.2 Half-Wave Plate Rotation, DC Bias at 0 and 100 V**

The percent modulation graphs show several interesting characteristics of the modulator setup. (Figures 10 & 11) First, the maximum percent modulation obtained with the RF signal is around 90%, corresponding to an extinction ratio of about 10:1. This is lower than the extinction ratio measured with the half-wave plate of 75:1. Possible causes for this difference are as follows; the input RF signal might not have enough amplitude to obtain half-wave voltage, piezoelectric resonances in the crystals may be interfering with the modulation, losses in the cables may decrease the amount of voltage across each successive crystal, internal capacitances in the modulator do not allow the electric field to reach a minimum, or some combination thereof. Second, the percent modulation curve for 0 V DC Bias appears periodic over 90 degrees while

the percent modulation curve for 100 V DC Bias appears less symmetric with maxima occurring approximately 45 degrees apart (Figures 10 & 11). A possible explanation for this behavior is that the 100 V bias is less than the half-wave voltage; therefore, the light through the crystals will be elliptically polarized. The RF signal into the modulator would change the polarization to and from elliptical polarization, giving a more complex angular behavior. It would be interesting to plot the percent modulation curves over 0-200 V DC Bias in a later experiment.

### **5.3 DC Bias**

Manufacturer specifications as well as theoretical calculations indicated that the half-wave voltage of the modulator should be around 144 V. The finding of this experiment (Section 4.3) showed the half-wave voltage to be 114.7 V. This discrepancy cannot be accounted for by experimental error. Recalculating the half-wave voltage (Equation 2) using a 750 nm wavelength instead of 830 nm yields a half-wave voltage of 130.3 V, still not within error. Further investigation of this experiment is needed to correctly identify the problem.

### **5.4 General Conclusions**

This array of experiments showed that laser modulation at high frequencies is attainable with the ConOptics electro-optical modulator. Improvements in the optical and RF setups should give better modulation depth than achieved here.

### **5.5 Opportunities for Further Research**

The extension of this research to 714 MHz modulation should be the next step for evaluating the uses of pulsed laser modulation for NLC research. To do so would require an amplifier capable of high gain at 714 MHz as well as a fast oscilloscope to correctly record the waveform. The cables on the modulator should be suited to the frequency (1 ns for 714 MHz) as noted in Section

2. Optimizing the RF setup for maximum modulation should also be attempted at 714 MHz. Finally, a more in-depth study of the DC Bias and its affects on the modulation behavior should be done. A constant crossed polarizer optical setup would greatly simplify the analysis of said study.

## **Acknowledgements**

I would like to thank my mentor Axel Brachmann for the patience he has had with me and with this project. He taught me a great deal about lasers and optics and also helped me to have fun while I was here. Thanks also go to the distinguished lecturers that kept my mind busy with thoughts of theoretical physics. Additionally, I would like to thank the Stanford Linear Accelerator Center and Department of Energy for having such a wonderful internship program as SULI.

## Literature Cited

- [1] T.B. Humensky, R. Alley, A. Brachmann, M.J. Brown, G.D. Cates, J. Clendenin, J. deLamare, J. Frisch, T. Galetto, E.W. Hughes, K.S. Kumar, P. Mastromarino, J. Sodja, P.A. Souder, J. Turner, M. Woods, *SLAC's Polarized Electron Source Laser System and Minimization of Electron Beam Helicity Correlations for the E-158 Parity Violation Experiment*, SLAC-PUB-9381.
- [2] The NLC Design Group. *Zeroth-Order Design Report for the Next Linear Collider*, SLAC-R-0474-VOL-1, May 1996
- [3] Hecht, Eugene. *Optics, Third Edition*. Addison-Wesley, Reading, Massachusetts, 1998. See pp. 363-366.
- [4] Koechner, Walter. *Solid State Laser Engineering, Third Edition*. Springer-Verlag, Berlin, 1992. See pp. 454-456
- [5] *Laser Modulation*, [http://www.conoptics.com/Laser\\_Modulation.htm](http://www.conoptics.com/Laser_Modulation.htm).
- [6] Enscoe, Robert F., Kocka, Richard J. *Electro-Optic Modulation: Systems and Applications*, [http://www.conoptics.com/Accessories\\_TechData.htm](http://www.conoptics.com/Accessories_TechData.htm).